Large Signal Simulation of Integrated Inductors on Semi-Conducting Substrates

Wim Schoenmaker, Michael Matthes, Bart De Smedt, Sascha Baumanns, Caren Tischendorf, Rick Janssen

***Abstract*—We present a formulation of transient field solving that allows for the inclusion of semiconducting materials whose dynamic responses are prescribed by drift-diffusion modeling. The robustness and the feasibility is demonstrated by applying the scheme to compute accurately the large-signal response of an integrated inductor.**

I. Introduction

The most common way to address electromagnetic (full-wave) field problems is by solving the Maxwell equations, i.e. setting up and solving discretized versions of these equations for the electric field $\mathbf{E}$ and the magnetic field $\mathbf{B}$. Moreover, another common ingredient is to solve the equations in the frequency regime. Faraday's law then provides a reduction of unknowns in the discretization using edge elements. The finite-integration technique does not attempt to reduce grid variables and therefore, these variables are a very faithful representation of the continuous degrees of freedom. In the transient regime, the latter has therefore been very successful in comparison to transient field solving based on finite-element methods and generalizations thereof. However, in semiconductor physics, the electric and magnetic fields are coupled to the carrier concentrations in a highly non-linear fashion. This is because the carrier densities depend on the *energy* density via the Boltzmann distribution functions, whereas the fields refer primarily to *forces*. The path dependency of the energy, being a force integrated along some path, will highly complicate the full-wave field solving if semiconductors are involved. This explains that so far, most semiconductor device simulators ignore the magnetic field because in this approximation, the force integral becomes path independent again. Fortunately, there is an appealing solution to avoid above complications. When the EM field problem is solvable in terms of the scalar potential and the vector potential, then it is possible to insert these solutions into the semiconductor equations and one has obtained a very straightforward upgrading of the semiconductor device simulation tools into the EM wave regime. In the last decade, we have demonstrated that, at least in the frequency domain, this solution is not only feasible but also leads to accurate results using standard non-linear and linear solver techniques [1]. This is not at all evident since the potential field formulation leads at first instance to a singular operator that needs to be regularized by gauge fixing. At the same time, the choice of the gauge fixing should not affect the outcome of physical variables such as resistance, inductance, capacitance, etc. The gauge independence of the physical variables is the outcome of a subtle interplay between the differential-geometry based discretization, the formulation of the boundary conditions and the selection of the gauge condition [2]. The potential field formulation requires only one grid (the 'primary grid') to be built. The scalar and vector potentials are located at the primary grid. The dual grid is a 'conceptional' tool to make the proper differential-geometry identifications.

Wim Schoenmaker and Bart De Smedt are with MAGWEL NV, Martelarenplein 13 B-3000 Leuven, Belgium email: wim@magwel.com, bart.desmedt@magwel.com

Michael Matthes, Sascha Baumanss and Caren Tichendorf are with University of Cologne, Mathematical Department Weyertal 86-90, Cologne, Germany email: mmatthes@math.uni-koeln.de, sbaumann@math.uni-koeln.de, tischendorf@math.uni-koeln.de

Rick Janssen is with NXP Semiconductors High Tech Campus 46 Eindhoven, Netherlands email: rick.janssen@nxp.com

978-3-9810801-8-6/DATE12/

II. Need for Mimetic Formulation

Just as in the frequency regime, the formulation of the transient equations for the potential fields are also subject to gauge fixing and differential-geometry based discretization considerations. Moreover, in the transient regime it becomes also evident that Gauss' law is not a dynamical evolution equation but a constraint, meaning that after each time step the state space vector should be compliant with this constraint. This is illustrated in Fig. 1. On the other hand in general the gauge condition can be time dependent, for example the Lorenz gauge. It can therefore play a role as part of the evolution equations. In this paper we will provide the complete and correct formulation of the transient equations for the potential fields which is fully compliant with mimetic principles [3]. Moreover, we show that standard linear (CGS) and non-linear solvers (Newton-Raphson) can be used to unfold the time evolution. The method is applicable to metallic materials that are covered by Ohm's law as well as semiconducting materials for which drift and diffusion contributions determine their voltage responses.

III. Field Equations

We start from the Maxwell equations in the potential formulation in the time domain. Then the Maxwell equations in these variables become:

For insulators:

$$-\nabla\cdot\left[\varepsilon\left(\nabla V+\frac{\partial\mathbf{A}}{\partial t}\right)\right]=0 \tag{1}$$

$$\nabla\times\frac{1}{\mu}\left(\nabla\times\mathbf{A}\right)=-\varepsilon\frac{\partial}{\partial t}\left(\nabla V+\frac{\partial\mathbf{A}}{\partial t}\right) \tag{2}$$

for conductors:

$$-\nabla\cdot\sigma\left(\nabla V+\frac{\partial\mathbf{A}}{\partial t}\right)=\frac{\partial}{\partial t}\left(\nabla\cdot\varepsilon\left(\nabla V+\frac{\partial\mathbf{A}}{\partial t}\right)\right) \tag{3}$$

$$\nabla\times\frac{1}{\mu}\left(\nabla\times\mathbf{A}\right)=-\sigma\left(\nabla V+\frac{\partial\mathbf{A}}{\partial t}\right)-\varepsilon\frac{\partial}{\partial t}\left(\nabla V+\frac{\partial\mathbf{A}}{\partial t}\right) \tag{4}$$

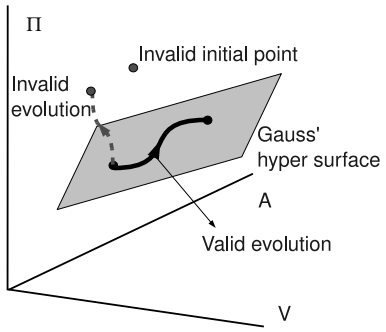

Fig. 1. 'Artist impression' of the Gauss' law-induced constraint for the time evolution of the full wave variables.

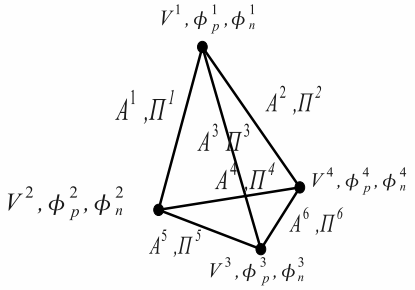

Fig. 2. Illustration of the discrete variables in one mesh cell

Besides the usual full-wave equations in the potential formulation for metals and insulators we find
for semiconductors:

$$-\nabla \cdot \frac{\varepsilon}{q}\left(\nabla V + \frac{\partial \mathbf{A}}{\partial t}\right) \quad = \quad p - n + N_{\rm dop} \tag{5}$$

$$p = n_i \, \mathrm{e}^{\frac{q}{kT}(\phi_p - V)} \quad , \quad n = n_i \, \mathrm{e}^{\frac{q}{kT}(V - \phi_n)} \tag{6}$$

$$\mathbf{J}_p = q\mu_p n_i \left[\mathrm{e}^{\frac{q}{kT}(\phi_p - V)}\left(\nabla V + \frac{\partial \mathbf{A}}{\partial t}\right) - kT\,\nabla \mathrm{e}^{\frac{q}{kT}(\phi_p - V)}\right] \tag{7}$$

$$\mathbf{J}_n = q\mu_n n_i \left[\mathrm{e}^{\frac{q}{kT}(V - \phi_n)}\left(\nabla V + \frac{\partial \mathbf{A}}{\partial t}\right) + kT\,\nabla \mathrm{e}^{\frac{q}{kT}(\phi_p - V)}\right] \tag{8}$$

The hole current-continuity equation is with U the recombination/generation :

$$\nabla \cdot \mathbf{J}_p = -U(n,p) - \frac{\partial p}{\partial t} \;\; , \;\; \nabla \cdot \mathbf{J}_n = U(n,p) - \frac{\partial n}{\partial t} \tag{9}$$

The Maxwell-Ampere equation becomes

$$\nabla \times \frac{1}{\mu}\left(\nabla \times \mathbf{A}\right) = \mathbf{J}_p + \mathbf{J}_n - \varepsilon \frac{\partial}{\partial t}\left(\nabla V + \frac{\partial \mathbf{A}}{\partial t}\right) \tag{10}$$

Finally, one needs to provide a *gauge condition:*

$$\frac{1}{\mu}\,\nabla\left(\nabla \cdot \mathbf{A}\right) + \epsilon \nabla\left(\frac{\partial V}{\partial t}\right) = 0$$

Due to the full-wave nature of the problem, there are *second*-order time differentiations. We circumvent these 2^{nd}-order differentiations in time by (1) applying a Legendre transformation to obtain the canonical momentum $\mathbf{\Pi} = \partial \mathbf{A}/\partial t$ conjugate to the vector potential field variable and (2), by putting *two* variables on each link of the primary grid, i.e. besides the usual projections of the vector potential on the links of the computational grid also the canonical momentum is projected on this grid and for each link it becomes an additional unknown (degree of freedom). Finally, since we have transformed the 2^{nd}-order time differentiation into a first-order one we use backward Euler time stepping. The remaining variables V, ϕ_p and ϕ_n are discretized in the conventional way: these discrete variables are placed on grid nodes. In Fig. 2, the variables are shown for one mesh cell. The presence of semiconducting materials requires that the currents in these regions need to be discretized using the Scharfetter-Gummel discretization method. The presence of the vector potential implies that the transient current becomes :

$$J_{ij} = \mathbf{J} \cdot \mathbf{n} = s^c \mu \, \frac{\Delta A}{h_{ij}} \left(c_i B[s^c \, X_{ij}] - c_j B[-s^c \, X_{ij}]\right) \tag{11}$$

where μ is the carrier mobility, $\mathbf{n}$ is the unit vector along the link $< ij >$ between nodes i and j and ΔA is the dual area corresponding to the link $< ij >$ whereas h_{ij} is the length of the link $< ij >$. The sign factor s^c is $+1$ for holes and -1 for electrons. The carrier density $c_{i,j} = p_{i,j}$ for holes and $n_{i,j}$ for electrons respectively in the nodes i and j. The argument of the Bernoulli function $B(x) = \frac{x}{\mathrm{e}^x - 1}$ is $X_{ij} = \frac{q}{kT}(V_j - V_i + s_{ij}\,\Pi_{ij} h_{ij})$. Finally $s_{ij} = \pm 1$, depending on the orientation of the link $< ij >$ with respect to its intrinsic orientation. It should be noted that the full system of equations still is redundant despite the fact that the gauge condition is added to regularize the singular (non-invertible) property of the curl-curl operator. The divergence of the Maxwell-Ampere equation leads to the current conservation law, and therefore, the latter is an implicit result after having found a solution of the first one. Alternatively, one may still insist on having the current-continuity equation(s) as part of the full set of equations that needs to be solved. In that case, one must omit the gauge condition as an independent equation to be solved. The gauge condition will be respected as an additional result from solving Gauss' law, the current-continuity equation and the Maxwell-Ampere equation. In fact, the elimination of the redundancy can also be lifted by using either the gauge conditions as a temporal evolution equation or Gauss' law as a constraint on the state variables at the latest time instance. All this is achieved provided that the mimetic principle is respected in the discretization method. The differential-geometry discretization scheme guarantees that either choice implies the other. The reader may wonder why introducing the gauge condition since it may be avoided after all in solving the transient problem. The reason for the inclusion of the gauge condition is found in the fact that the transient problem may have a static solution. In that case one runs into the singular character of the curl-curl operator. Therefore, the gauge condition still is needed for regularization of this operator. Details of the corresponding discretization procedure can be found in [4].

IV. Application

We demonstrate the feasibility of the method by computing the on-set transient response of the current flow that is induced in the substrate (semiconductor) by switching on the voltage from 0 to 1 Volt in 100 ps. The structure is shown in Fig. 3 and is isolated from the substrate by 2.48 micron of dielectric consisting of several layers. Integrated inductors are a key-component for RF circuits such as low-noise amplifiers (LNA), voltage controlled oscillators (VCOs), filters and impedance matching networks. In Monolithic Microwave Integrated Circuits (MMICs), inductors still occupy a significant portion of the total area. Furthermore, integrated inductors can induce parasitic couplings. In order to prevent and limit such disturbing couplings, special attention should be paid to placement and radiation-optimization of integrated inductors. Planar spiral inductors, while offering scalable layout canonical architectures (rectangular, octagonal) with ease of manufacturing suffer from low Q-factors. During the last years, considerable efforts have been directed towards finding ways to design inductors with increased quality factors and higher resonant frequencies. The shown 8-shaped configuration [5], compared to classical rectangular, octagonal, circular topologies, has the advantage of limiting EMC (Electro-Magnetic Compatibility) related issues when symmetrical structures are considered. The EMC reduction is expected to result from the twisted nature of the 8-shaped topology, where the two constitutive loops will lead to equal magnetic field distributions with opposite polarities [6], [7]. Here a design improvement is highlighted to

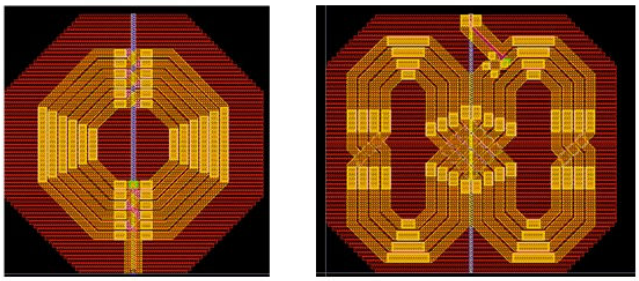

Fig. 3. Octagonal (left) and 8-shaped (right) VCO coil

show the difference between an octagonal coil and an 8-shaped coil. Fig. 3 shows the octagonal and 8-shaped coil used for a VCO. Fig. 4 gives the measurement results of the 2fm spur (in dBc) at the RF output as a function of the output power (Pout). The main graph (VCO-octagonal coil) shows that the spur is above the -40dBc, which is the upper level that is acceptable. Use of the VCO 8-shaped coil improves the spurious level by 10dB. Using 8-shaped coils, the quality factor and the self-inductance (L) of the coil will de-crease only slightly, depending on the situation. Refer to Figure 5. The inductor is designed in M6-M7-M8. The substrate thickness is 100 micron and is equipped with a ground contact at the back (not shown in Fig. 6) and is p-type doped with a value of 10^15cm^{-3}. The full simulation domain is shown in Fig 7. Note that a layer of air is included to allow for the electromagnetic field spread around the inductor. The structure is discretized using a grid of 52185 nodes leading to 330983 variables in the linear systems

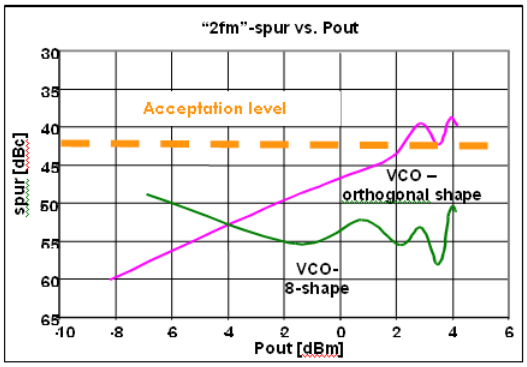

Fig. 4. Measurement of spur level of octagonal and 8-shaped coil

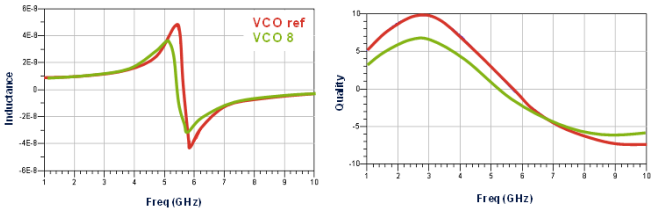

Fig. 5. Inductance and quality factor of octagonal (red) and 8-shaped (green) coil

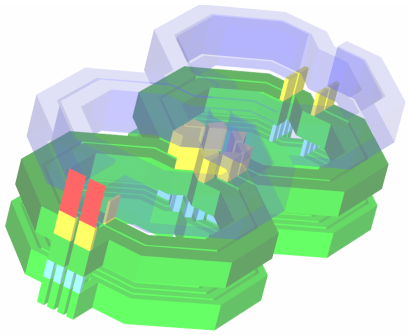

Fig. 6. View of the integrated 8-shaped inductor from above. The vertical direction is stretched

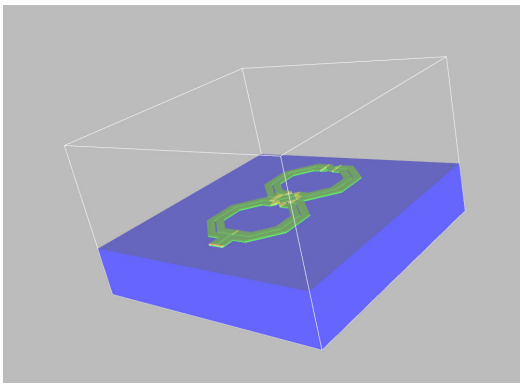

Fig. 7. View of the full simulation domain

of the Newton-Raphson scheme needed to solve the implicit next time step problem. We performed a time stepping of 1 ns in 10 intervals with a step function potential change at one of the inductor contacts. A capacitive coupling to the substrate is detected and its strength as well as the inductance of the on-chip inductor can be extracted from the results. In Fig. 8, the currents into and out of the inductor contacts are shown. In Fig. 9, the transient current in the ground plane contact is

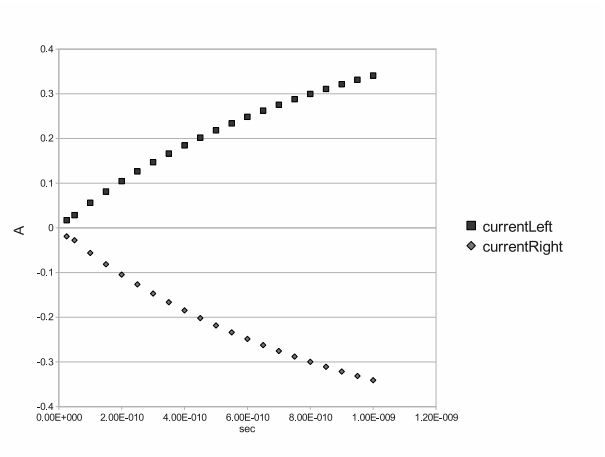

Fig. 8. Value of currents at the left and right contact of the inductor

shown. An overshoot effect is observed. In Fig. 10, the current of the ground plane contact is shown in a logarithmic plot. Clearly, two time constants are observed. The corresponding 'signal-decay' constants are (1) for 0-4 nsec: $1.5 \times 10^{10} sec^{-1}$ and (2) for 4 - 10 nsec: $0.48 \times 10^{9} sec^{-1}$. In general the

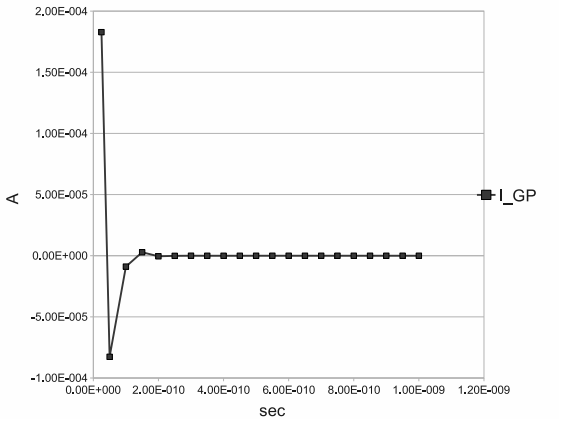

Fig. 9. Value of the current in the ground plane contact. A transient overshoot is observed

advantage of having a transient design flow in place is to circumvent the problems arising from using frequency domain EM models (S-parameters) in transient circuits. Often these S-parameter models turn out to have a lack of passivity and stability, resulting in transient solutions not converging, arising from failing to capture dominant poles in the right frequency plane. For this approach, as an example, the 8-shaped inductor can be used by comparing a simple circuit with a simple

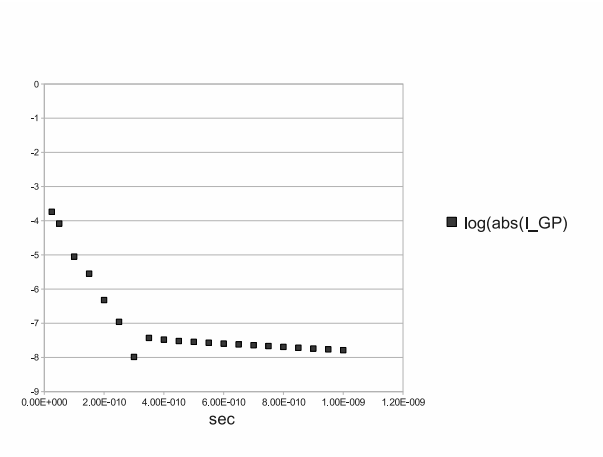

Fig. 10. Logarithm of the absolute values of the current in the ground-plane contact. Two time scales are observed.

lumped element inductor model in transient with the same circuit coupled with the EM model. In order to assess the results of the current build-up shown in Fig. 8, we represent the inductor as a simple lumped compact model (see Fig. 11), consisting of L, R and C to ground. As a first approximation we can take the values from the RF-simulations which give a value of 3 Ω at 1 GHz, but in order to get a good fit, we took R=2 Ω. Using a step magnitude of 1.0 Volt, the result in Fig. 12 is obtained. The need for this fitting already indicates that the RF values that were obtained with the assumption of small-signal perturbations can not be assumed to be the correct values if large signals are applied. The current build-up is shown to be in good agreement with the currents in Fig. 8.

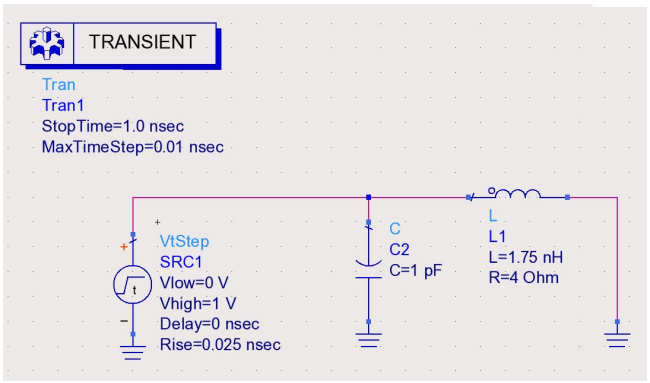

Fig. 11. Set up of a compact model for the transient results.

Beside the constant time step solutions presented before, we realized and tested a variable time step and variable order implementation of the backward differential formulas (BDF), also known as the implicit Gear formulas, see [8]. It is particularly suited for stiff ordinary differential equation systems and widely used for transient circuit simulation, e.g. in all SPICE based circuit simulation packages. After space discretization of the electromagnetic field equations (1)-(10),

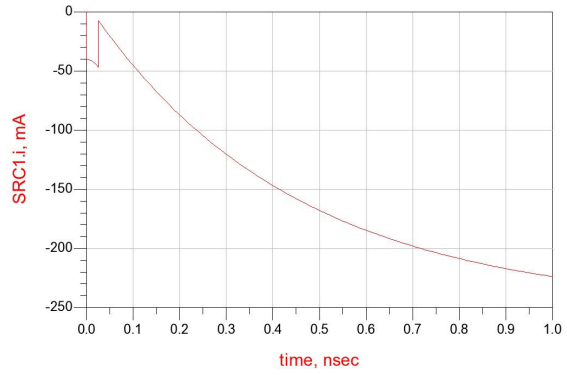

Fig. 12. Results of a compact model for the transient simulation using a step magnitude of 1Volt.

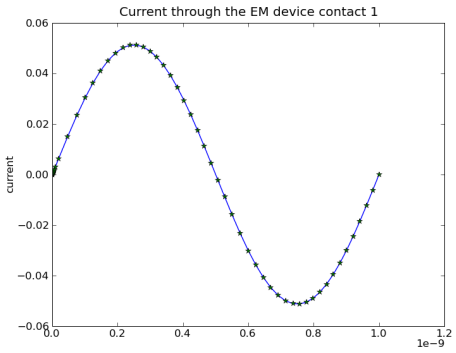

Fig. 13. Current through the first contact of the 8-shaped inductor after transient simulation with variable order and variable time step size.

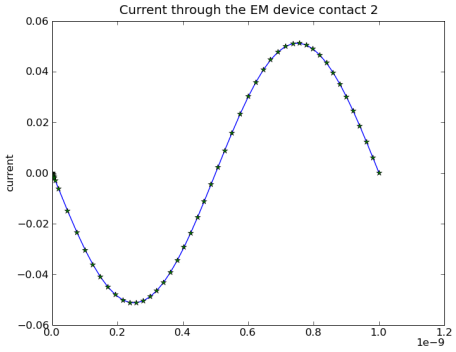

Fig. 14. Current through the second contact of the 8-shaped inductor after transient simulation with variable order and variable time step size.

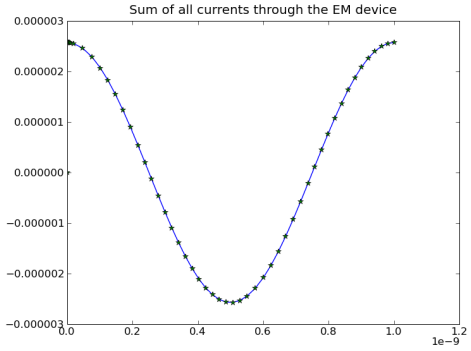

Fig. 15. Sum of all simulated currents (including the substrate current) through the 8-shaped inductor after transient simulation with variable order and variable time step size.

we obtain an ordinary differential equation system of the form

$$g(\frac{\mathrm{d}^2u(t)}{\mathrm{d}t^2}, \frac{\mathrm{d}u(t)}{\mathrm{d}t}, u(t), t) = 0$$

with $u(t)$ involving the vector potential field variables $\mathbf{A}(t)$ for each link of the primary grid, the nodal potentials $V(t)$ at each node of the primary grid as well as the electron density $n(t)$ and the hole density $p(t)$ at each node of the primary grid belonging to semiconducting material, all evaluated at the time point t. Using the canonical momentum $\mathbf{\Pi} = \partial\mathbf{A}/\partial t$ we arrive at a first order system of the form

$$f(\frac{\mathrm{d}w(t)}{\mathrm{d}t}, w(t), t) = 0 \tag{12}$$

with $w(t)$ including $u(t)$ as well as $\mathbf{\Pi}(t)$ at each link of the primary grid.

Applying the BDF methods of order k with variable time steps τ_n to (12), we obtain an equation system of the form

$$f(\frac{1}{\tau_n}\sum_{i=0}^{k}\alpha_{ni}w_{n-i}, w_n, t_n) = 0 \tag{13}$$

with certain time step dependent coefficients α_{ni}. For determining the numerical approximation w_n of $w(t_n)$ we solve the nonlinear equation system (13) by Newton's method. As reported before, we have to solve a linear equation system of dimension 330983 for each Newton step. Since the resulting Newton matrix is positive definite having nonzero entries on the diagonal, we used the algebraic multigrid package SAMG [9] for a memory saving and time efficient solution of these systems.

Figures 13 and 14 show the transient results for the 8-shaped inductor when a sinusoidal voltage with 1 GHz frequency is applied between the first and the second contact. The variable stepsize was automatically selected by a predictor - corrector based error estimation guaranteeing an error of the magnitude of 10^{-4}. Figure 15 shows two nice results of the quality of our simulation. First, the numerical discretization preserves charges (the sum of all currents through the 8-shaped inductor is almost zero). Secondly, the global error is smaller than 3×10^{-6}, i.e. the prescribed error tolerance has been reached.

V. Conclusions

In this paper we presented a large-signal field solving approach that faithfully represents semiconducting material responses. The method exploits a Legendre transformation on the full-wave formulation such that we can apply standard backward Euler differential methods for adaptive time integration. Furthermore, we have incorporated Gauss' law as a constraint that should be respected at all time instances. The gauge condition results 'for free' once the solution is

obtained. We demonstrated the correctness of the method by applying it to an industrial design problem, i.e. by computing the large-signal response of an integrated inductor above a semi-conducting substrate. The transient information provides complementary insight in the behavior of complex designs in which electromagnetic interaction can jeopardize the 'first-time-right' EDA goal. In particular, RF modeling in the frequency domain is limited to the small-signal response superpositioned to a fixed operation point. Transient simulations are not limited to the perturbative nature of the stimuli and therefore are a valuable add-on to improve virtual prototyping.

VI. Acknowledgments

This work is supported by the EU project ICESTARS. /FP7/2008/ICT/21214911

References

[1] W. Schoenmaker et al. *Evaluation of Electromagnetic Coupling between microelectronic Device Structures using Computational Electrodynamics* Proceedings Scientific Computing in Electrical Engineering SCEE2008, pp. 61-65, Eds. Janne Roos and Luis R.J. Costa, Springer Verlag.

[2] W. Schoenmaker et al. *Modeling of Passive-Active Device Interactions* Proceedings ESSDERC 2007, pp. 163-166, Munich Germany Eds. Doris Schmidt Landsiedel and Roland Thewis, IEEE, 2007.

[3] K. Lipkinov , J. Morel and M. Shashkov *Mimetic finite difference methods for diffusion equations on non-orthogonal non-conformal meshes* Journal of Computational Physics, Vol. 199, 2004

[4] Quan Chen, Wim Schoenmaker, Peter Meuris and Ngai Wong "An Effective Formulation of Coupled Electromagnetic-TCAD Simulation for Extremely High Frequency Onwards" IEEE Trans. on Computer-Aided Design of Integrated Circuits and Systems, vol. 30 Issue: 6, pages: 866 - 876, 2011

[5] J. Einziger, "Planar inductance", Patent # WO 2004/012213, 5 February 2004

[6] O. Tesson, "High Quality Monolithic 8-Shaped Inductors for Silicon RF IC Design", IEEE Topical Meeting on Silicon Monolithic Integrated Circuits in RF Systems (SiRF 2008)

[7] B. Fahs, P. Gamand and C. Berland, "Low-phase-noise LC-VCO using high-Q 8-shaped inductor" , Electronics Letters, Vol. 46, No. 2, 2010

[8] C. W. Gear, "Simultaneous Numerical Solution of Differential-Algebraic Equations" , IEEE Trans. Circuit Theory, Vol. CT-18, No. 1, pp. 89-95, 1971

[9] U. Trottenberg and T. Clees "Multigrid Software for Industrial Applications - From MG00 to SAMG" In Notes on Numerical Fluid Mechanics and Multidisciplinary Design, E. Hirschel and E. Krause (eds.), Springer Berlin/Heidelberg, Vol. 100, pp. 423-436, 2009

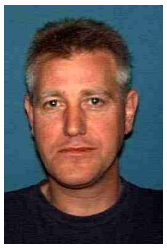

Wim Schoenmaker, received his B.Sc. and M.Sc. degree in Physics from the Free University of Amsterdam in 1975 and 1979 in theoretical physics, and his Ph.D. degree in theoretical high-energy physics from the University of Groningen in 1983. He held post-doctoral positions in particle physics at the University of Kaiserslautern (Germany) and the University of Leuven (Belgium), where his research interests concerned lattice gauge theories and statistical physics and computing. From 1987 until 2003 he was at the Interuniversity Microelectronic Center (IMEC) at Leuven, working on the development of CAD tools. From 1993-2003 he was heading the Technology CAD group at IMEC. From 1998-2005, Wim Schoenmaker was an associate editor of the IEEE Transactions on Computer-Aided Design. In 2003, he co-founded the company MAGWEL that provides software solutions for the simulation of interconnects and integrated passives on the medium and high-frequency range. He is CTO of MAGWEL (2003-present). Wim Schoenmaker is the (co-) author of 140 peer-reviewed journal papers and conference contributions, and three patents and 1 book and 2 book chapters.

Michael Matthes studied Mathematics and Economathematics at the University of Cologne and at the University of St Andrews. He received his diploma in Mathematics from the University of Cologne in 2008. Currently he is a Ph.D. student at the University of Cologne and his research interests include the numerical analysis of Differential-Algebraic Equations (DAEs) and the simulation and analysis of coupled systems of partial differential equations and DAEs in circuit simulation.

Bart De Smedt received the M.Sc degree in electrical engineering from the Katholieke Universiteit Leuven, Leuven, Belgium in 1995. He became a research assistant at the MICAS division and developed novel methodologies for design space exploration and yield-aware synthesis for analog and RF circuits. In 2003 he co-founded Kimotion Technologies, a start-up developing EDA tools for analog yield-aware synthesis. At the merger with Magwel in 2008 he became part of Magwel's product development team. Currently his major focus is on R&D activities in the domain of power transistor modeling and simulation, applied in Magwel's extraction tools.

Sascha Baumanns received his diploma in Mathematics from the University of Cologne (Germany), in 2008. He has been a teaching assistant and PhD student at the group of Mathematics/Numerical Analysis in Cologne. His research interests include field/circuit coupling and numerical analysis of differential-algebraic equations (DAEs).

Caren Tischendorf received her PhD (1996) and her Venia Legendis (2004) in mathematics from Humboldt University of Berlin. Beside her main employment at the Humboldt University of Berlin, she has been working as guest researcher at the Scientific Centre of IBM in Heidelberg, at the Centre for Research and Development of SIEMENS in Munich and at the Numerical Analysis Dept. of Lund University in Sweden as well as visiting professor at the Technical University of Berlin. Since 2006 she is Professor for Mathematics/Numerical Analysis at the Mathematical Institute of the University of Cologne. Her main fields of research activity are circuit and device simulation, numerical analysis of differential-algebraic equations (DAEs) and partial differential equations (PDEs) as well as coupled systems. Teaching is mostly focused on introductory and advanced courses in numerical analysis and simulation. She is member of the Scientific Advisory Committee of the SCEE (Scientific Computing in Electrical Engineering) conferences.

Rick Janssen graduated from the University of Nijmegen, the Netherlands, in Theoretical Physics in 1983. He subsequently did his PhD there in 1988. He then joined Philips in the Mathematical Software Group of the Centre for Manufacturing Technology in Eindhoven, doing promotion and support of mainly in-house developed electromagnetic simulation software. In 1991 this group became part of the Applied Mathematics Group of the central Philips Research Laboratories in Eindhoven, where he became responsible for the support on electromagnetic modelling in general and of electromagnetic simulation packages, both in-house developed and Vector Fields software in Philips world-wide. He now is a member of the Physical Design Methods group of NXP Central R&D, where he is a Senior Scientist, participating in RF and EM simulation and consultancy projects.